Iraqi National Journal of Earth Science

www.earth.mosuljournals.com

Investigation of Petrophysical Properties of Butmah Formation (Early Jurassic) Using Well Logs of Selected Wells, Northern Iraq

Maha. M. Al-Dabagh [1*], Irfan Sh. Asaad [2]

[1] *Petroleum Reservoir Engineering Department, College of Petroleum and Mining Engineering, University of Mosul, Iraq.*

[2] *Department of Earth Sciences and Petroleum, College of Science, University of Salahaddin -Erbil, Kurdistan Region, Iraq.*

Article information

Received: 27- Jan -2024

Revised: 14- Mar -2024

Accepted: 14- Apr -2024

Available online: 01- Jan – 2025

Keywords:
Early Jurassic
Butmah
Petrophysical Properties
Porosity
Hydrocarbon Saturation
Northern Iraq

Correspondence:
Name: Maha. M. Al-Dabagh

E-mail
mahamuneeb@uomosul.edu.iq

ABSTRACT

Petrophysical properties of the Early Jurassic Butmah Formation are investigated in three wells (Kand-1, Kd-1; Sheikh Adi-1B, SA-1B; and Shaikan-5B, Sh-5B), in northern Iraq. The data from the well logs are digitized using NeuraLog software, and they were evaluated using Interactive Petrophysics (IP) software. The lithological cross-plots show that the Butmah Formation is mainly comprised of limestone, dolomitic limestone, and dolomite with shale and anhydrite layers. Comparing the wells, it becomes clear that the Butmah Formation in well (Kd-1) has a low effective porosity in the first zone and some depths in the third zone, while it has a higher effective porosity in the first and second zones of wells (Sh-5B) and (SA-1B). Due to the presence of shale, microporosity, and anhydrite cement, the sonic porosity (matrix porosity) has increased at several depth intervals, especially in the (Sh-5B) and (SA-1B) wells. Five permeable zones have been determined based on the permeability curves for the Sh-5B and SA-1B wells. The limited permeability of the Butmah Formation is mostly attributed to the presence of anhydrite cement and shale, whereas the high permeability may be caused by fractures, particularly opened fractures, as well as other factors including the shape and tortuosity of the pores. The presence of shale layers and cement hurts all the petrophysical characteristics in the Butmah Formation, especially in the (Kd-1) well. However, when a reservoir unit is present beneath these beds, they may serve as a good seal or cap. The hydrocarbon saturation (Sh) results from this study show that the (SA-1B) well exhibits high hydrocarbon saturation compared to the (Sh-5B) well.

DOI: 10.33899/earth.2024.146079.1218,

دراسة الخصائص البتروفيزيائية لتكوين البطمة (الجوراسي المبكر) باستخدام المجسات البئرية لآبار مختارة شمالي العراق

مها منيب الدباغ [1]* ، عرفان شعبان أسعد [2]

[1] قسم الهندسة المكامن النفطية، كلية هندسة النفط والتعدين، جامعة الموصل، الموصل، العراق.

[2] قسم علوم الأرض والنفط، كلية العلوم، جامعة صلاح الدين-أربيل، إقليم كردستان، العراق

معلومات الارشفة

تاريخ الاستلام: 27- يناير -2024

تاريخ المراجعة: 14- مارس -2024

تاريخ القبول: 14- ابريل -2024

تاريخ النشر الالكتروني: 01- يناير -2025

الكلمات المفتاحية:

الجوراسي المبكر

بطمه

الخصائص البتروفيزيائية

المسامية

التشبع الهايدروكاربوني

شمالي العراق

المراسلة:

الاسم: مهى منيب الدباغ

E-mail: mahamuneeb@uomosul.edu.iq

الملخص

فُحصت الخصائص البتروفيزيائية لتكوين بطمة (الجوراسي المبكر) في آبار قند-1 (kd-1) وشيخان (Sh-5B) وشيخ عادي (SA-1B) شمالي العراق. تم تحويل بيانات المجسات البئرية الى صيغة رقمية باستخدام برنامج (NeuraLog) وتقييمها باستخدام برنامج (Interactive Petrophysics). أظهرت مخططات التقاطع الصخرية ان تكوين بطمة يتألف بشكل أساسي من الحجر الجيري، والحجر الجيري المتدلمت، والدولومايت فضلا عن طبقات الطَفَل والانهايدرايت. مقارنة مع البئرين الاخرين، تبين ان بئر (Kd-1) يمتلك قيم معتدلة للمسامية الفعالة، لا سيما في النطاق الثاني وبعض أجزاء النطاق الثالث من تكوين بطمة. من جهة أخرى، تبين ان بئري (Sh-5B) و (SA-1B) يمتلكان قيماً عالية للمسامية ضمن النطاقين الأول والثاني من التكوين. نتيجة لوجود الطَفَل والمسامية الدقيقة والسمنت الانهايدرايتي، فان المسامية المحسوبة من المجس الصوتي تزداد عند بعض أعماق بئري (Sh-5B) و (SA-1B). واعتماداً على منحنيات النفاذية لهذين البئرين، فقد قسم التكوين الى خمسة أنطقة. ويعتقد ان سبب انخفاض النفاذية في تكوين بطمه يعود الى وجود الطين والسمنت الانهايدرايتي، في حين تمثل الكسور السبب الرئيس للنفاذية العالية، ولا سيما المفتوحة منها، فضلا عن عوامل أخرى كشكل المسامات ومساراتها المنحنية. ان وجود الطبقات الطفلية والسمنت في التكوين ولا سيما في بئر قند-1 لها تأثير سلبي على الخصائص البتروفيزيائية كافة. وعليه، تعمل هذه الطبقات كصخور حاجزية او غطاء للوحدات المكمنية الواقعة اسفلها. وأظهرت النتائج أن التشبع العالي للهايدروكاربونات ظهر في بئر (SA-1B) مقارنة ببئر (Sh-5B).

DOI: 10.33899/earth.2024.146079.1218,

Introduction

The hydrocarbon significance of Jurassic rocks in northern Iraq has increased in recent years. This is visualized with newly discovered oil fields in the Kurdistan region of Iraq, where Jurassic and Cretaceous rocks acted as reservoirs, particularly in Shaikhan, Swara-Tuka, Atrush, Bakrman, Mirawa, and Bina-Bawi oilfields (Verma *et al.*, 2004) as well as the Jurassic rich shale formations that are considered as significant source rocks for hydrocarbon in Iraqi Territory, as Sargelu Formation (Aqrawi *et al.*, 2010). The commonly considered Jurassic reservoir units in northwestern Iraq include the Butmah, Mus, and Alan formations (Price et al., 2020). The Early Jurassic Butmah Formation, which is selected for the present study, exists only in subsurface sections in the south, middle, and northwest of Iraq (Jassim *et al.*, 2006). It was first introduced by Dunnington in 1953 in Butmah -2 well northwest Mosul City (Bellen *et al.*, 1959). Lithologically, the Butmah Formation in its type locality is divided into three sections: 200 m of oolitic, pseudo-oolitic, and detrital limestone with beds of argillaceous limestone, shale, and anhydrite in the upper part; 180 m of oolitic and pseudo-oolitic limestone, argillaceous, and dolomitic with sandstone and shale beds in the middle; and 120 m of limestone with bedded anhydrite in the lower part (Jassim *et al.*, 2006). The Formation, which belongs to the Early Liassic period (Jassim *et al.*, 2006) gradually and laterally interfingers with the Sarki

Formation toward northeastern Iraq (Buday, 1980; Csató *et al.,* 2014). It is expected to be deposited in sabkha settings and a shallow lagoon with somewhat high salinity (Jassim *et al.,* 2006; Csató *et al.,* 2014; Kddo and Nader, 2014). Local Early Jurassic reservoirs within the Butmah Formation produce minor oil at the Atshan field, and minor hydrocarbon is recorded in Adaiyah-1, Makhul-2, Najmah-29, and Ibrahim-1 wells (Jawzi and Associates, 2005).

The three open-hole oil exploration wells that are selected for the current study involve Kand-1 (Kd-1) located 33 km northwest of Mosul City in the Low Folded Zone; Shaikan-5B (Sh-5B) 58 km northeast Mosul City, and Sheikh Adi-1B (SA-1B) 48 km northeast Mosul City. The last two wells are located in the area where the Low-Folded and High-Folded zones meet (Fig.1 and Table 1).

The Butmah Formation reservoir description in Shaikan-1B and Atrush-1 wells, Kurdistan Region was examined by Zangana et al. (2020). Another study was done by (Mohammed Sajed and Glover, 2020) on the reservoir quality of the Butmah Formation in Butmah and Ain Zalah oilfields in north-western Iraq. According to well-log interpretation, (Ali *et al.*, (2022) identified the separated vugs, matrix (interparticles), and fractures as the three key forms of porosity in the formation.

Table 1: latitude and longitude for the three studied wells

Well Name	Latitude	Longitude
Kd-1	36° 39' 53" N	43° 01' 37" E
Sh-5B	36° 47' 43" N	43° 30' 43" E
SA-1B	36° 48' 51" N	43° 12' 01" E

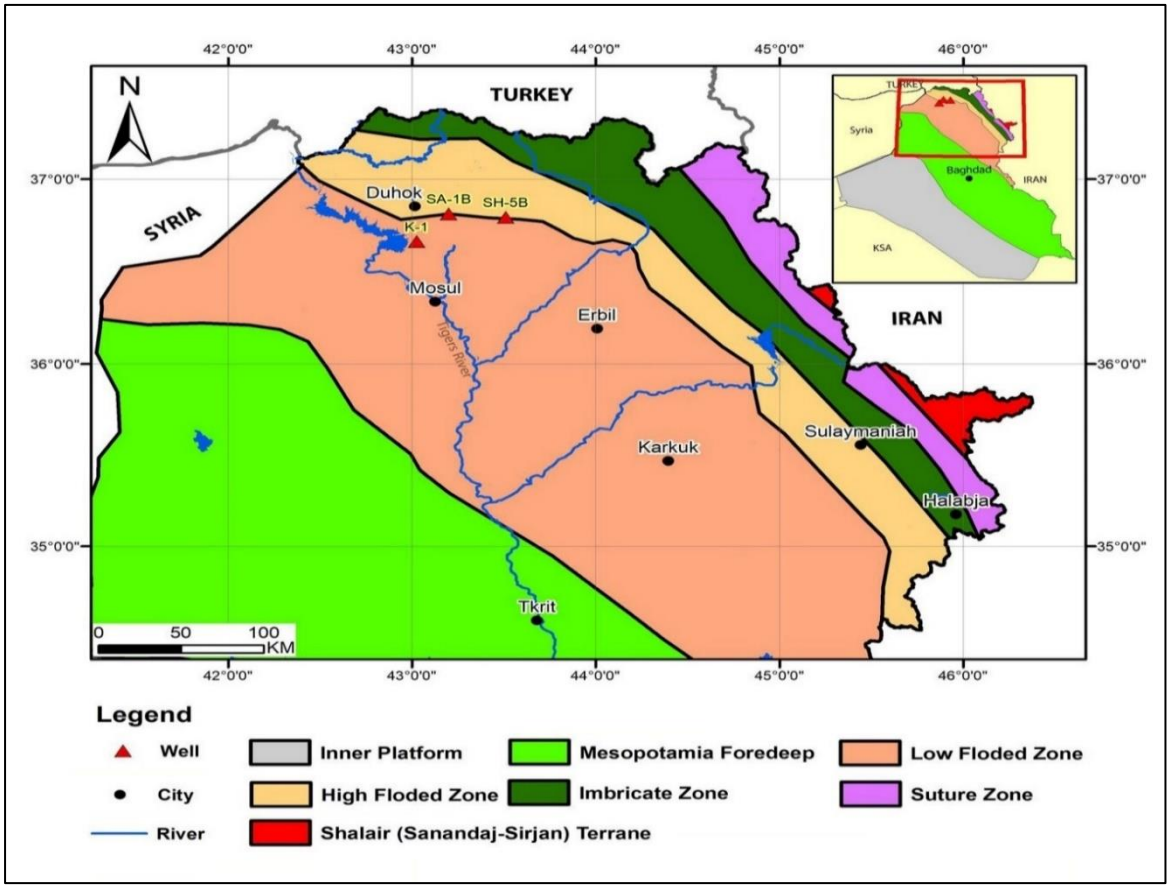

Fig. 1. Location of the studied wells in northern Iraq with the tectonic divisions of Iraq (after Fouad, 2015).

Aim of Study

Generally, petrophysical characteristics of the Butmah Formation have not been the subject of many studies. It may be due to the high heterogeneity in the formation rocks. The primary aim of the current study is a quantitative evaluation of the petrophysical properties and prediction of the hydrocarbon presence in the Butmah Formation in (Kd-1, SA-1B, and Sh-5B) wells in the northern part of Iraq using well logs data.

Material and Methods

Three open-hole oil wells are available to investigate the petrophysical properties of the Butmah Formation. Well logs for Sh-5B and SA-1B are obtained from Hattingh et al. (2015). The well environmental effects are corrected by Gulf Keystone Petroleum (GKP), while logs for (Kd-1) are obtained from the North Oil Company (Table-2). Utilizing NeuraLog software, the wireline log data for the wells Kand-1 (Kd-1), Sheikh Adi-1B (SA-1B), and Shaikan-5B (Sh-5B) are converted to digital format. This software converts scanned images into LAS files, which are then loaded into the IP software (IP V3.5, 2008). Interactive Petrophysics V.3.5 is used for well-log calculations and interpretations, such as the shale volume, lithology, porosity, permeability, and fluid saturation. In addition to the neutron-density and M-N cross-plots, the lithology interpretation of the Butmah Formation is based on the resistivity, sonic, gamma-ray, caliper, and neutron-density composite logs. Finally, litho-saturation plots are used to display the variation in petrophysical characteristics and lithology vertically.

Table 2: Available log data for Butmah Formation

Well Name	Depth Interval (m) from R.T.K. B	Available Well Log Data
Kd-1	2421-2909	CAL, GR, RHOB, NPHI, and DT.
Sh-5B	1310-2010	CAL, GR, RHOB, NPHI, RDEP, RMED, and RMIC
SA-1B	1732-2162	CAL, GR, RHOB, NPHI, RDEP, RMED, and RMIC

Results

The lithology and other petrophysical characteristics of an oil borehole can be continuously tracked using well logs. Three wells are investigated petrophysically in the present study. Lithology, porosity, permeability, and hydrocarbon saturation are the four petrophysical characteristics that have been estimated.

1. The Shale Volume (V_{sh}) Determination:

Determining the volume of shale is crucial since it greatly affects both fluid saturation and effective porosity. The following formula for older rocks from the gamma-ray index (IGR) equations can be used to calculate the volume of shale in formation (Vsh) from a gamma-ray log (Larionov, 1969) and (Schlumberger, 1989):

$$I_{GR} = \frac{GR_{log} - GR_{min}}{GR_{max} - GR_{min}} \quad \text{..... (1)}$$

$$V_{sh} = 0.33 * (2^{2 * I_{GR}} - 1) \quad \text{..... (2)}$$

where:

I_{GR} = gamma ray index, GR_{log} = gamma ray reading of formation, GR_{min} = minimum gamma ray (clean carbonate), GR_{max} = maximum gamma ray (shale), V_{sh} = volume of shale for rocks older than Tertiary.

The current study subdivides the Butmah Formation into three petrophysical zones based on the curves for the volume of shale (Tables 3 and 4 and Fig.2).

Table 3: The shale volume values of the three zones in the Butmah Formation.

Well Name	Depth Intervals (m)		
	Zone-1	Zone-2	Zone-3
Kd-1	(2421-2590)	(2590-2678)	(2678-2909)
Sh-5B	(1310-1505.5)	(1505.5-1665)	(1665-2010)
SA-1B	(1732-1840)	(1840-1942)	(1942-2162)

Table 4: The three zones in the Butmah Formation's shale volume values.

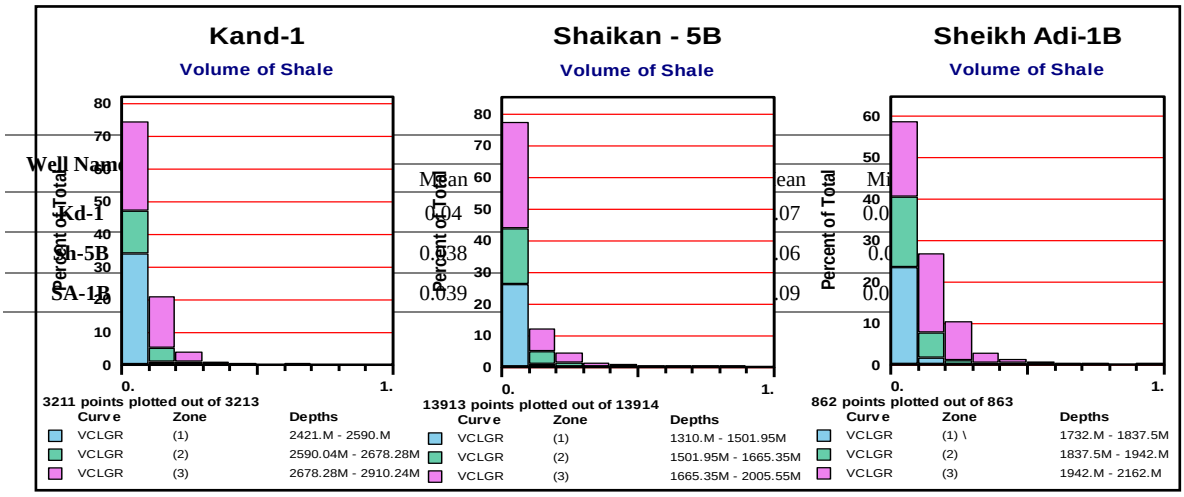

Fig. 2. Shale volume histograms in the studied wells for Butmah Formation.

2. Determination of Lithology and Mineralogy:

The lithology of the reservoirs can be estimated using gamma-ray and SP logs, as well as a combination of two or three different porosity logs, such as neutron, density, and sonic logs. Because of the varied lithology in the Butmah Formation, the current study has used the cross-plot method to identify the rock types:

- **Neutron- Density Cross-plot**

Because it gives accurate results compared to other types, the pair of neutron and density measurements are used to assess lithology and porosity (Fig. 3).

- **MN Cross-plot**

The density, neutron, and compressional sonic logs are used by the M-N cross-plot to determine the lithology using quantities of M and N (Schlumberger, 1972) (Fig.4). The terms M and N are defined as follows:

$$M = \frac{\Delta t_f - \Delta t_{log}}{\rho_b - \rho_f} * 0.01 \quad \ldots\ldots\ldots\ldots\ldots\ldots\ldots\ldots\ldots\ldots (3)$$

$$N = \frac{\emptyset_{Nf} - \emptyset_N}{\rho_b - \rho_f} \quad \ldots\ldots\ldots\ldots\ldots\ldots\ldots\ldots\ldots\ldots (4)$$

where:

Δtf = fluid transit time, Δtlog = interval transit time (from the log), ρb = bulk density (from the log), ρf = fluid density (= 1.1gm/cc), $Ø_{Nf}$ = neutron porosity of the fluid of the formation (usually =1) and ØN = neutron porosity (from the log).

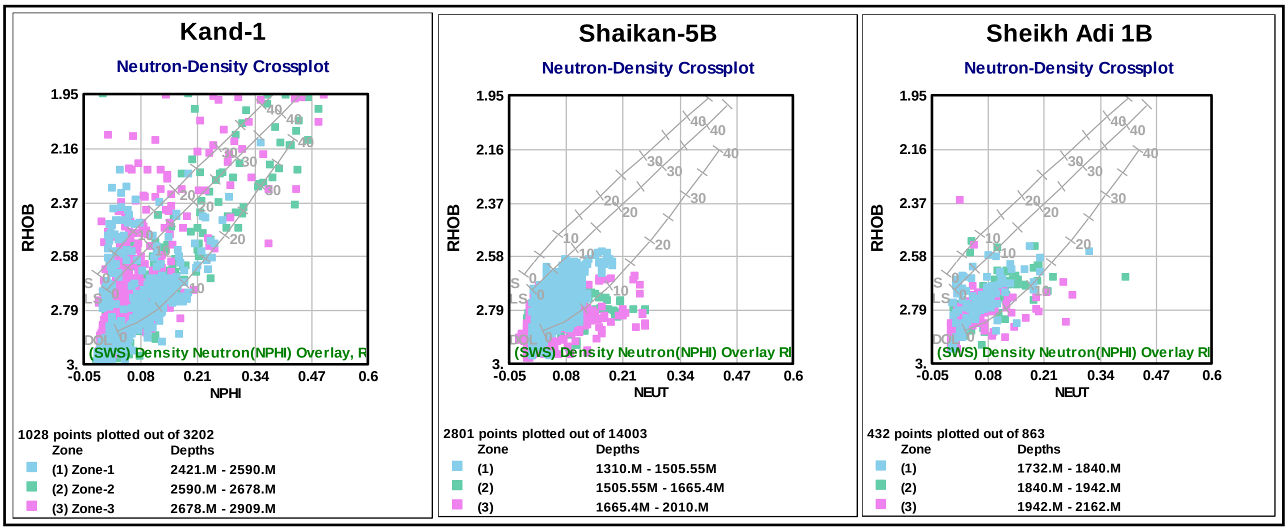

Fig. 3. The Butmah Formation's Neutron-Density cross-plots in the studied wells

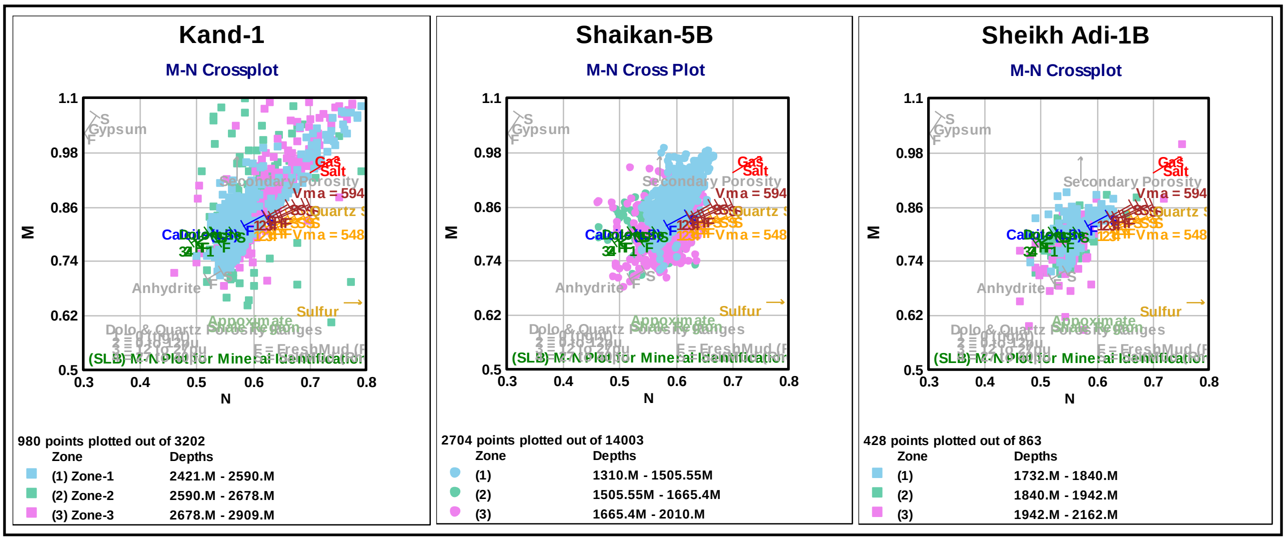

Fig. 4. The Butmah Formation's M-N Cross-plots in the studied wells

3. Porosity Determination

Pore volume is the area available for the storage of water and hydrocarbons in oil and gas reservoirs. For measuring the porosity of the Butmah Formation's reservoir, conventional density, neutron, and sonic logs are employed.

- **Total Porosity:**

Neutron-density derived porosities were combined to obtain the total porosity of the Butmah Formation. After lithology effect correction, the neutron log assesses the direct porosity. The porosity from the density log can be found using the following formula:

$$\mathbf{ØD} = \frac{(\rho \mathbf{ma} - \rho \mathbf{b})}{(\rho \mathbf{ma} - \rho \mathbf{f})} \quad \ldots\ldots\ldots\ldots\ldots\ldots\ldots\ldots\ldots\ldots\ldots\ldots \text{(5)}$$

where:

ØD = porosity from density log, ρb = bulk density recorder by log, ρ_{ma} = density of the dry rock (= 2.71 g/cm^3 for limestone, 2.86 g/cm^3 for dolomite), ρf = density of fluid (= 1.1 g/cm^3).

To obtain accurate results, the following equations must be used to correct density and neutron porosities from the shale effect (Taib and Donalson, 2004):

$$ØNC = ØN – (Vsh * ØNsh) \quad \text{…… (6)}$$

$$\emptyset \boldsymbol{D_C} = \left(\frac{\boldsymbol{\rho_{ma}-\rho_b}}{\boldsymbol{\rho_{ma}-\rho_f}}\right) - \boldsymbol{V_{sh}} * \left(\frac{\boldsymbol{\rho_{ma}-\rho_{sh}}}{\boldsymbol{\rho_{ma}-\rho_f}}\right) \quad \text{……... (7)}$$

where:

ØNsh = shale porosity from neutron, ρsh = shale's bulk density.

Next, the total porosity (Øt) is computed as follows:

$$\emptyset_t = \frac{\emptyset_{Nc}+\emptyset_{Dc}}{2} \quad \text{…….. (8)}$$

- **Effective Porosity**

After subtracting the shale volume from the total porosity, the effective porosity is calculated using the formula of Schlumberger (1989) (Fig. 5) and (Fig. 6) and (Table 5):

$$Øe = Øt \times (1 - Vsh) \quad \text{……... (9)}$$

Table 5: The values of effective porosity for the three zones in the Butmah Formation.

Well Names	Effective Porosity for Zone-1			Effective Porosity for Zone-2			Effective Porosity for Zone-3		
	Min.	Max.	Mean	Min.	Max.	Mean	Min.	Max.	Mean
Kd-1	0	0.407	0.077	0	0.476	0.142	0	0.401	0.073
Sh-5B	0	0.154	0.037	0	0.104	0.030	0	0.116	0.019
SA-1B	0	0.193	0.043	0	0.199	0.058	0	0.120	0.027

- **Primary and Secondary Porosity:**

The pore space that develops during the initial settle down of a sediment is known as the primary porosity. Primary porosity is classified into two basic categories: intragranular, also known as intraparticle, and intergranular or interparticle. By definition, secondary porosity is developed after a sediment is deposited (Selley, 2000). Compared to primary porosity, secondary porosity has a wider variety of morphologies and a more complicated genesis. It is found in carbonate rocks more often than in siliciclastic sands (Choquette and Pray, 1970). For the Butmah Formation, the sonic log is applied to calculate primary or matrix porosity using the following formula when the shale volume ranges between (10-34) %:

$$ØSc = ØS - \left(\boldsymbol{V_{sh}} \times \frac{\boldsymbol{\Delta t_{Sh}-\Delta t_{ma}}}{\boldsymbol{\Delta t_f - \Delta t_{ma}}}\right) \quad \text{…….....} \quad (11)$$

The following formula is applied when the volume of shale is above 35% (Dresser Atlas, 1979):

$$ØSc = \left(\boldsymbol{ØS} \times \frac{\boldsymbol{100}}{\boldsymbol{\Delta t_{sh}}}\right) - \left(\boldsymbol{Vsh} \times \frac{\boldsymbol{\Delta t_{Sh}-\Delta t_{ma}}}{\boldsymbol{\Delta t_f - \Delta t_{ma}}}\right) \quad \text{.....} \quad (12)$$

where:

Δt_{ma} = Interval Transit Time in the Matrix 47.6 (μsec/ft) for limestone and 43.5 (μsec/ft) for dolomite, Δt_f= interval transit time in the fluid within the formation for saltwater mud 185 (μsec/ft), Δt_{log}= interval transit time in the formation (μsec/ft). Δt_{sh} = interval transit time in shale, Øs the porosity that is calculated using the following equation:

$$\emptyset_s = \frac{\boldsymbol{\Delta t_{log}-\Delta t_{ma}}}{\boldsymbol{\Delta t_f - \Delta t_{ma}}} \quad \text{……} \quad (13)$$

Finally, the difference between the total porosity and the predicted time-average behavior of carbonate rocks is known as the secondary porosity index, or SPI. (Fig.6). This SPI is attributed to the presence of vugs and fractures that are not detected by the sonic log (Schlumberger, 1974)

$$SPI = (Øt - ØSc) \quad \text{……} \quad (14)$$

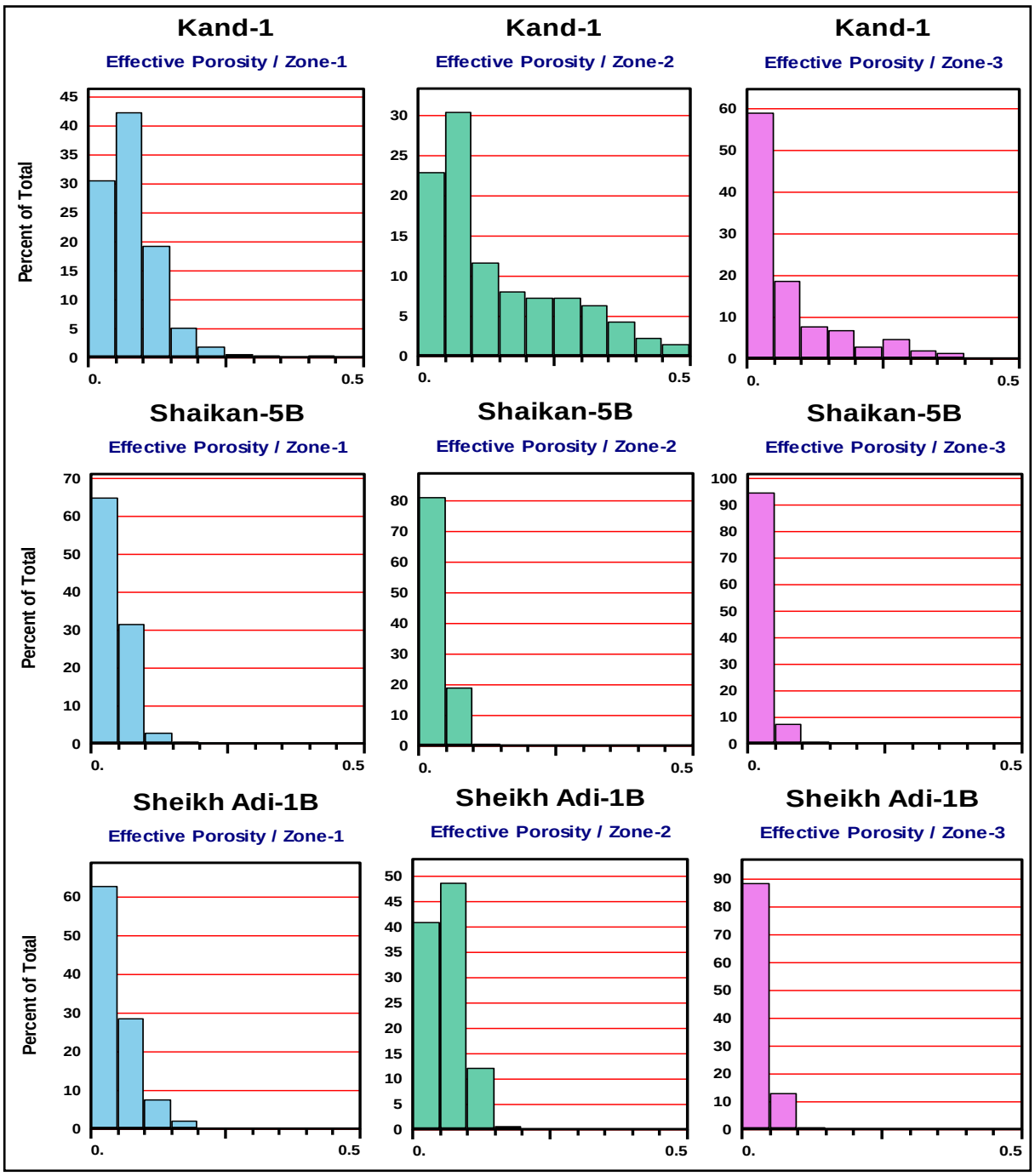

Fig. 5. Effective porosity histograms for the three-petrophysical zones of Butmah Formation in the studied wells

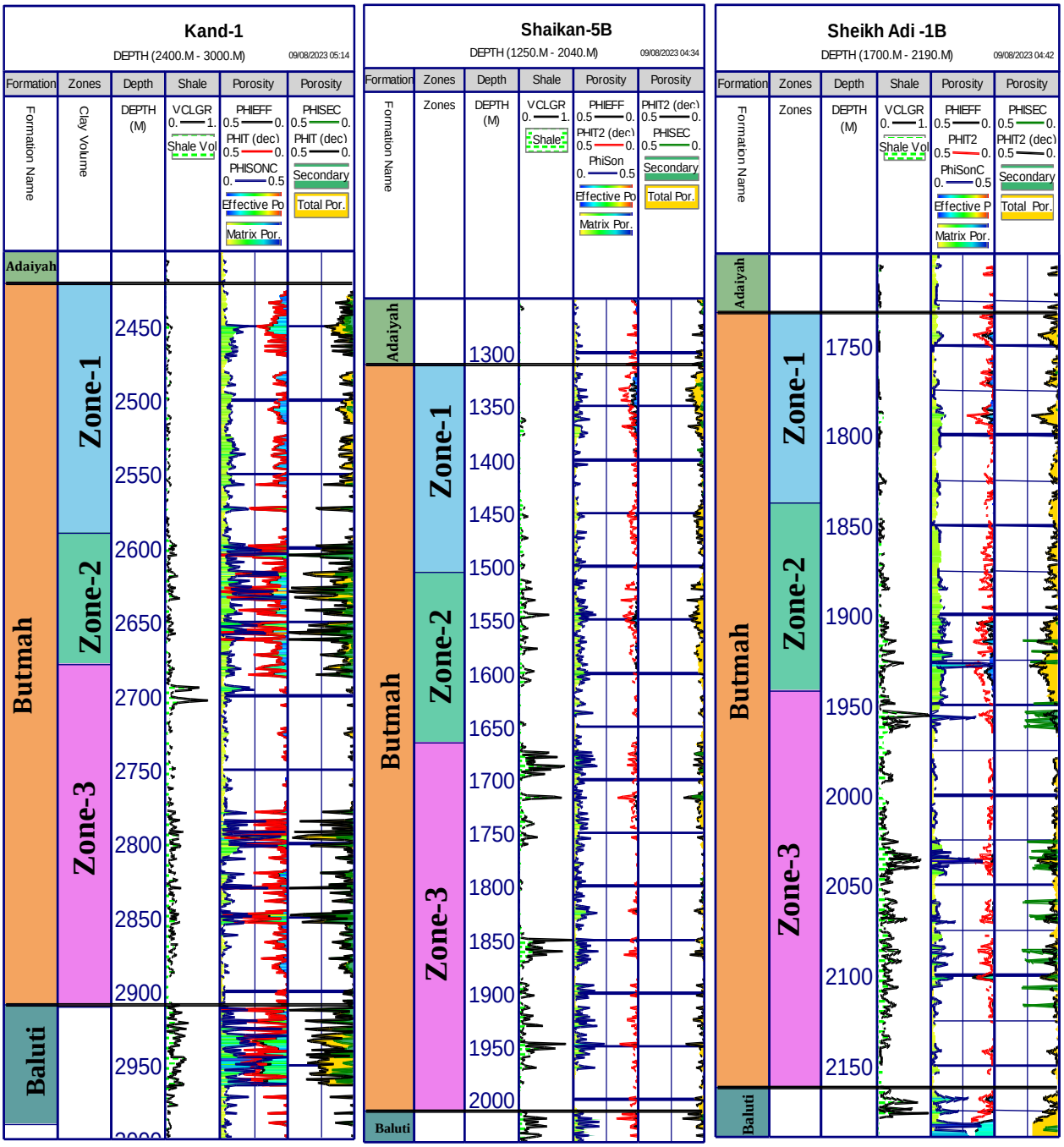

Fig. 6. The curves of shale volume and porosity types for Butmah Formation in the studied

4. Estimation of Water and Hydrocarbon Saturations

The following equation is used to determine the water saturation of the study area's wells, except the Kand-1 well due to the unavailability of resistivity log data (Archie, 1942):

$$S_w = \left(\frac{a \times R_w}{\emptyset^m \times R_t}\right)^{1/n} \quad \text{..... (15)}$$

where:

S_w = saturation of water, R_w = resistivity of the formation water, a = the tortuosity factor (= 1), m = the cementation exponent (= 2.04 in Sh-5B, = 1.95 in SA-1B (Hattingh *et al.*, 2015), n = saturation exponent (=2) (Hattingh *et al.*, 2015), R_t = true formation resistivity as derived from a deep resistivity log.

The formation temperature (T) in the area of study was used by the ERCE equation (Hattingh *et al.*, 2015):

$$T=27+0.02\times D \quad \ldots\ldots\ldots\ldots\ldots\ldots\ldots\ldots\ldots\ldots \quad (16)$$

where: D = Formation Depth.

The following equation is used for the estimation of the hydrocarbon saturation (Sh) (Figures 7 and 8) and (Table 6):

$$Sh = 1-Sw \quad \ldots\ldots\ldots\ldots\ldots\ldots\ldots\ldots\ldots\ldots\ldots\ldots \quad (17)$$

Due to a lack of information, particularly regarding the resistivity of the drilling fluid (R_{mf}), the current study just calculated the hydrocarbon saturation without defining the movable oil saturation (MOS) and residual oil saturation (ROS).

Table 6: The values of hydrocarbon saturation for the three zones in the Butmah Formation

Well Names	S_h for Zone-1			S_h for Zone-2			S_h for Zone-3		
	Min.	Max.	Mean	Min.	Max.	Mean	Min.	Max.	Mean
Sh-5B	0	0.930	0.595	0	0.826	0.392	0	0.898	0.356
SA-1B	0.001	0.914	0.667	0.019	0.885	0.508	0.022	0.896	0.546

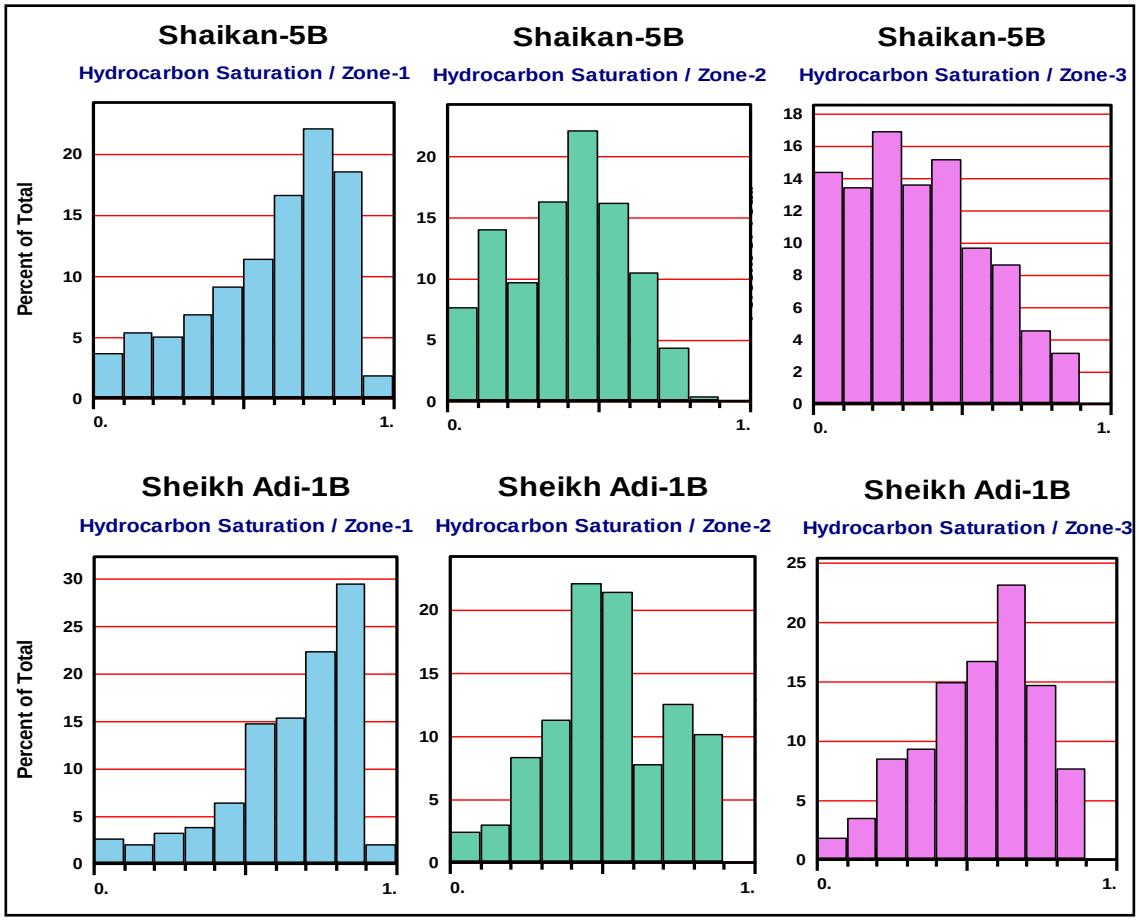

Fig.7. Hydrocarbon saturation histograms in the three-petrophysical zones of Butmah Formation at Sh-5B and SA-1B wells

5. Permeability Calculation

The permeability is determined from the well logs following the Schlumberger method. It only calculates the permeability for the (Sh-5B) and (SA-1B) wells because of the insufficient data, particularly the resistivity logs from the (Kd-1) well (Fig.8). To determine the absolute permeability, the Schlumberger chart (K-3) is used by the connection between effective

porosity (Φe) and irreducible water saturation (Swi) (Schlumberger, 1989). The permeability curves show five permeable zones (Figures 9 and 10) and (Tables 7 and 8).

$$K = 10000\ Øe\ 4.5/\ Swi\ 2 \quad \text{…….} \quad (18)$$

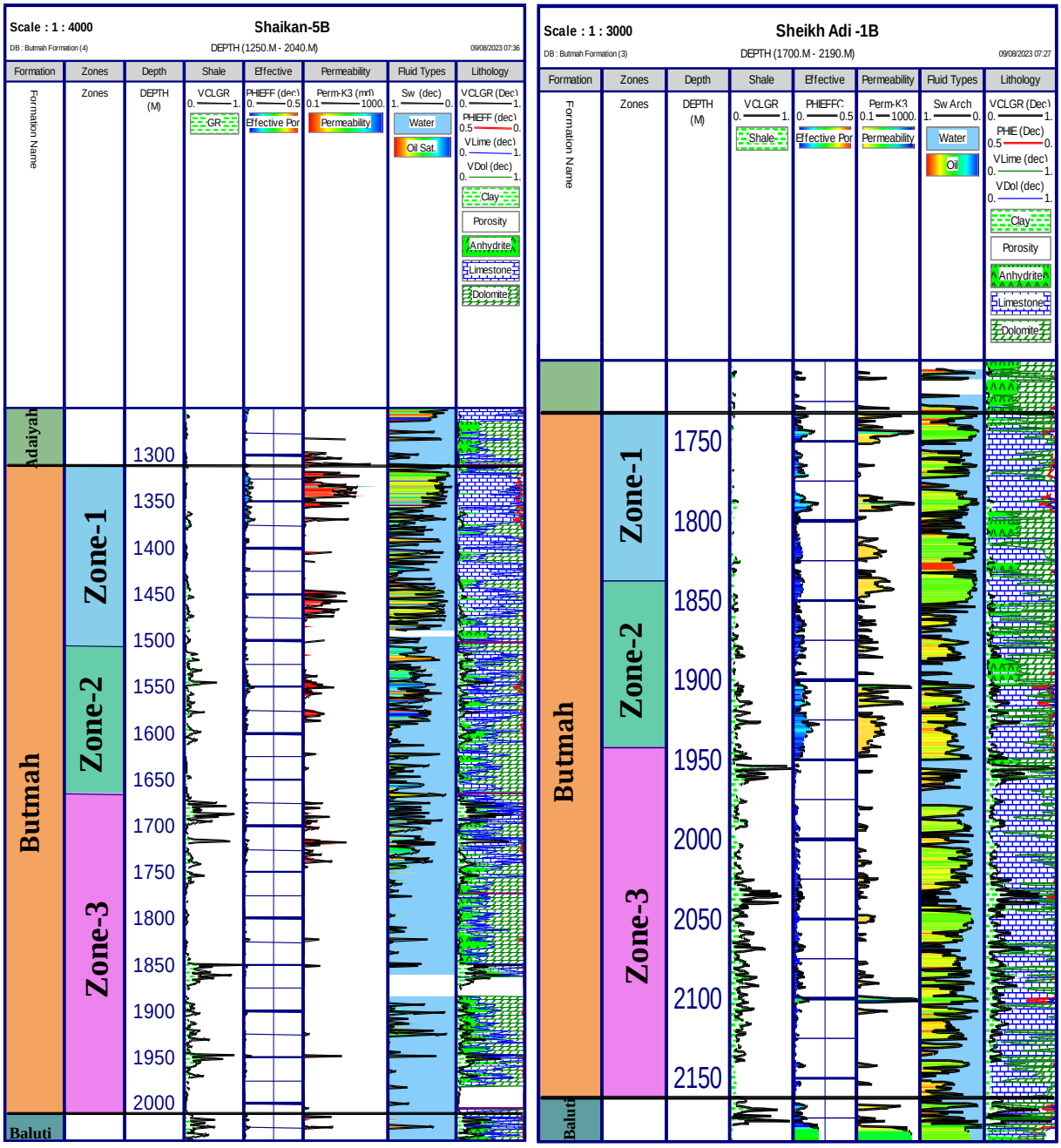

Fig. 8. Litho-Saturation crossplots in (Sh-5B) and (SA-1B) wells.

Table-7: Values of permeable zones in Butmah Formation at Shaikan-5B well.

Zone Names	Depth Intervals (m)	Permeability (mD)		
		Min.	Max.	Mean
1-A	1310-1371	0.010	473	2.98
1-B	1445.7-1473.6	0.011	14.43	1.05
2-A	1535-1559	0.012	3.12	0.37
2-B	1574-1588	0.012	1.17	0.35
3-A	1671-1741	0.010	10.66	0.34

Table-8: Values of permeable zones in Butmah Formation at Sheikh Adi-1B well

Zone Names	Depth Intervals (m)	Permeability (mD)		
		Min.	Max.	Mean
1-A	1730-1756	0.022	418	6.43
1-B	1786-1826	0.014	419	1.64
2-A	1830-1948	0.012	293	1.24
3-A	2012.5-2053	0.022	2.05	0.61
3-B	2093-2110.5	0.010	3376	9.13

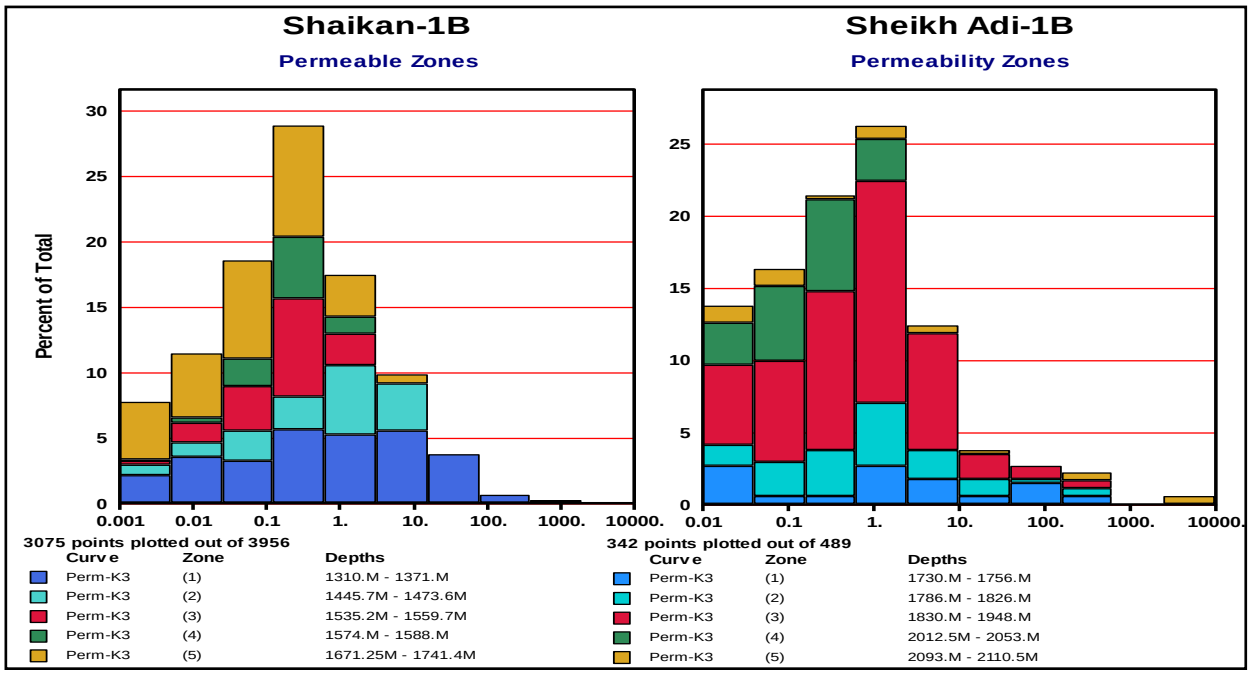

Fig. 9: Permeability histograms in the permeable zones of Butmah Formation in SA-1B and Sh-5B wells.

Discussion

Many studies found that the Shaikan and Sheik Adi oil fields contain hydrocarbons in the fractured carbonates of the Cretaceous, Jurassic, and Triassic intervals (GKP, 2010; Hattingh *et al.*, 2015; Price *et al.*, 2020). The Butmah Formation is an Early Jurassic formation made up of naturally fractured dolomite and limestone. The Shaikan 1-B well has heavy oil-bearing rocks separated from the younger Jurassic strata by anhydrite layers (95 m thick) that act as a barrier or seal to fluid flow (GKP, 2010).

Butmah Formation is subdivided into three petrophysical zones, named Zone-1, Zone-2, and Zone-3, and each has distinct petrophysical characteristics as mentioned in Table (3). The volumes of shale in these petrophysical zones are illustrated in Figure (2) and Table (4), where the mean values for three wells were (0.04 to 0.13), (0.038 to 0.10), and (0.039 to 0.17), respectively, in the Kd-1, Sh-5B, and SA-1B wells. In contrast to the other two zones, Zone-3 has higher shale values, particularly in the SA-1B well.

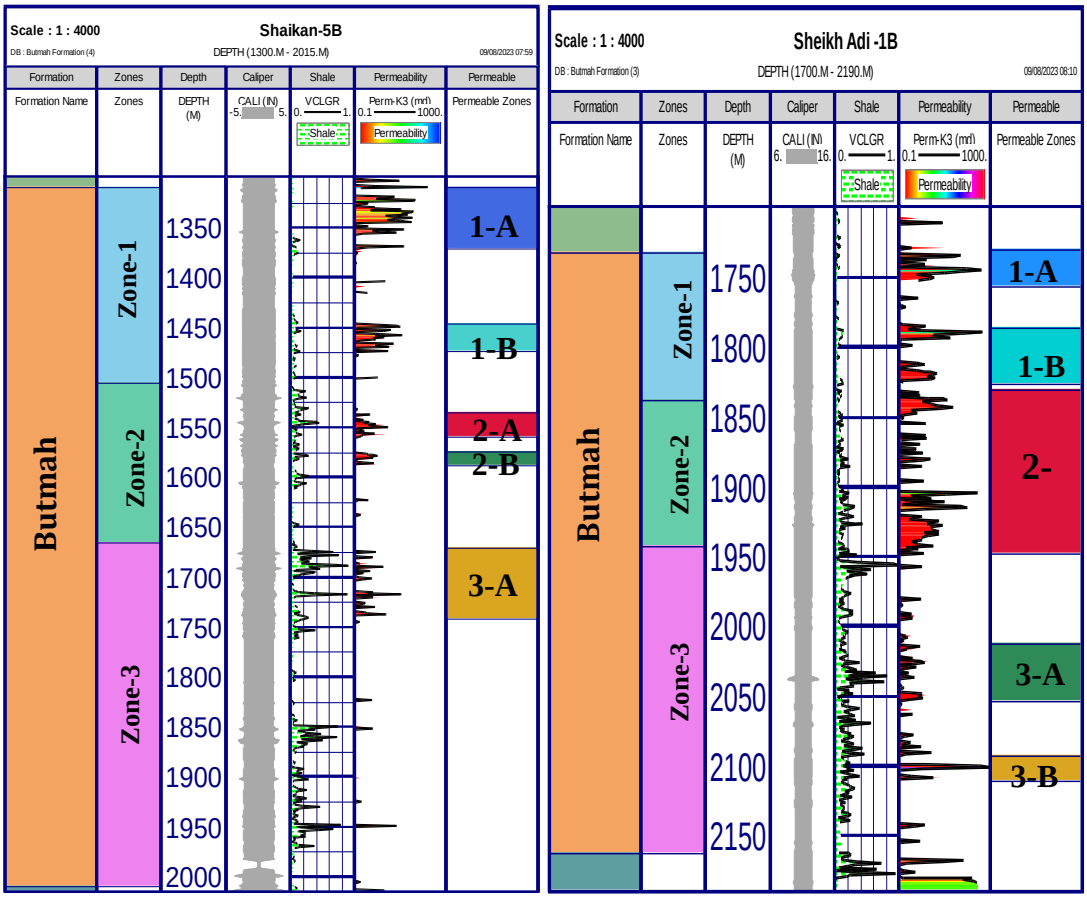

Fig. 10: The permeable zones of Butmah Formation in Sh-5B and SA-1B wells.

Lithological interpretation of the Butmah Formation is based on the neutron-density and M-N cross-plots in addition to gamma-ray, caliper, resistivity, sonic, neutron, and density curves. The findings show primary lithologies (limestone, dolomite, and dolomitic limestone with a few thin layers of anhydrite) of the three studied wells, while the shale, particularly in Zone-3, is represented by the points that are dispersed below the dolomite line and have high gamma ray readings (Figs.3 and 4). In addition to the aforementioned, the cross-plots show that there is sandstone that is interfering with shale in the three zones of the (Kd-1) well. There is a wide variety of effective porosity values in the studied wells shown in the entire analysis of effective porosity that is given in Figure (5) and Table (5). The average of the effective porosity ranges between (0.07 – 0.14), (0.01 – 0.03), and (0.02 – 0.05) in Kd-1, Sh-5B, and SA-1B wells respectively. In comparison to the other two wells, the (Kd-1) well has larger porosity values, particularly in Zone-2 and at some depths in Zone-3 of the Butmah Formation, whereas the (Sh-5B) and (SA-1B) wells have higher effective porosity values in Zone-1 and Zone-2 of the formation.

The primary porosity (matrix porosity) as determined by the sonic log calculations differs between the wells in the investigated area. The Butmah Formation's total porosity is lower in the majority of the formation in the (Kd-1) well, except for the anhydritic carbonate intervals, where the matrix porosity is higher (Fig.6). Whereas the (Sh-5B) and (SA-1B) wells demonstrate that there are several depths where matrix porosity is greater than the total porosity, resulting negative SPI values at these intervals. According to Schlumberger (1974, 1989), the SPI is influenced by the presence of vuggy and fractures porosity because the sonic log ignores these types of porosity and responds primarily to intergranular porosity. Other studies revealed that several factors including pore system geometry, the presence of spherical pores (such as oolitic molds), microporosity, interlaminar, and inter-peloidal porosities, which slow acoustic

velocities and lead to high sonic porosity values, may affect SPI (Brie *et al.,* 1985; in Anselmetti and Eberli, 1999; Soete *et al.,* 2015). Moldic pores cause an increase in P-wave velocities, which causes the moldic pores rocks to have higher velocities than micro moldic pores rocks (Soete *et al.,* 2015). The work suggests that the major sources of high matrix porosity in the (Sh-5B) and (SA-1B) wells are the presence of shale, anhydrite cement, and maybe microporosity in limestone and dolomite successions. Anhydritic cement and nodules have been suggested to be the cause of low total porosity values compared with high sonic porosity values in dolomite beds, particularly if that dolomite was formed by the seepage reflux model (Balaky *et al.,* 2023). The reflux dolomite with contemporaneous anhydrite cement is observed as anhydrite nodules associated with fine crystalline dolomite in the Butmah Formation in (Bm 15) well (Mohammed Sajed and Glover, 2020). Regarding this, (Mohammed Sajed et.al., 2022) referred to the early anhydrite fabrics are linked to the dolomitization of the Butmah Formation's tidal flat facies, which decreased the reservoir quality of the formation by occupying the early intercrystalline pores of the dolomitized units.

The empirical estimates of permeability using the Schlumberger chart (K-3) method show variable values of permeability. The current study categorizes the Butmah Formation into five zones based on the permeability curves for the Sh-5B and SA-1B wells as shown in Figures (9 and 10) and Tables (7 and 8). While the other zones in the formation have low permeability. Zone 1-A of the two wells and Zone 3-A of the SA-1B well have the best permeability. The presence of clay and cement, especially anhydritic cement, is thought to be the primary cause of the Butmah Formation's low average permeability. Mohammed Sajed and Glover (2020) suggest that a more dispersed porosity-permeability relationship in the Butmah Formation results from the early dolomitization associated with anhydrite cement. Despite having low average porosities, the formation's Zones 1-A and 3-B in the studied wells show high permeability, with maximum values ranging from (418-3376 mD). This may be due to existing fractures, especially opened fractures, as well as other variables like the pore's shape and tortuosity.

Except for the anhydrite and shale beds, the hydrocarbon saturation (Sh) resulting from this study shows that the (Sh-5B) well has good hydrocarbon saturation in Zones-1 (on average 0.59) and Zone-2 (on average 0.39) of the Butmah Formation, while the (SA-1B) well exhibits high hydrocarbon saturation throughout the formation (Table7 and Fig.7). Regarding this, Zangana et al. (2020) observed that the hydrocarbon in Butmah Formation concentrates in the upper part of the formation at Atrush-1 and Shaikan-1B wells. They also mentioned in their study that most of the movable hydrocarbon in both wells is similar to the residual hydrocarbon.

Conclusions

The Butmah Formation is classified into three petrophysical zones known as Zone-1, Zone-2, and Zone-3 based on its petrophysical characteristics. The log cross-plots show that the formation’s main constituents are limestone, dolomite, and dolomitic limestone, with layers of anhydrite and interfingering shale. Additionally, the (Kd-1) well contains thin sandstone layers that are intercalated with shale. Effective porosity averages in the Kd-1, Sh-5B, and SA-1B wells range from 0.07 to 0.14, 0.01 to 0.03, and 0.02 to 0.05 respectively. Generally, the lower values of effective porosity are associated with high values of volume of shale, especially in Zone-3. Due to the presence of shale, microporosity, and anhydrite cement, there are various depth intervals, especially in (Sh-5B) and (SA-1B) wells that show a rise in sonic porosity (matrix porosity).

There are five permeable zones in the Butmah Formation. The best permeable zones are zones 1-A in the (Sh-5B) and (SA-1B) wells and Zone 3-A in the SA-1B well, whereas the other zones have low permeability. Along with additional factors like pores' shape and tortuosity, the high permeability intervals may be linked to the formation's fractures, especially opened fractures. With average hydrocarbon saturation in zones 1 and 2 of the Butmah

Formation of 0.59 and 0.39, respectively, the (Sh-5B) well exhibits good hydrocarbon saturation. While all zones of the formation in the (SA-1B) well look to have significant hydrocarbon saturation. All petrophysical properties of the Butmah Formation, particularly in the (Kd-1) well, are negatively impacted by cement, especially anhydrite cement, and shale thin beds. These beds, however, can serve well as a seal or cap when a reservoir unit is situated beneath them.

Acknowledgments

In particular, we would like to thank the Iraqi North Oil Company for supplying the Kand-1 well data. Mr. Waad Sh. Asaad is appreciated for his kind computer facilities. Our thanks also extend to Mr. Andrew Logan and Mr. Koko Kyi petrophysicists from Thailand and Canada respectively for their advice on the current work.

References

Ali, M.A., Al-Dabagh, M.M. and Asaad, I. Sh., 2022. Determination of Porosity Types Impressive on Butmah Formation (Early Jurassic) in Selected Wells Northern Iraq (Case Study). AIP Conference Proceedings, 2443, 020003. https://doi.org/10.1063/5.0091917.

Anselmetti, F.S. and Eberli, G.P., 1999. The Velocity-Deviation Log: A Tool to Predict Pore Type and Permeability Trends in Carbonate Drill Holes from Sonic and Porosity or Density Logs. AAPG Bull., 83(3): pp. 450-466. https://doi.org/10.1306/00AA9BCE-1730-11D7-8645000102C1865D.

Aqrawi, A.A., Goff, J.C., Horbury, A.D. and Sadooni, F.N., 2010. The Petroleum Geology of Iraq. Scientific Press. 424 P.

Archie, G.B., 1942. The Electrical Resistivity Log as an Aid in Determining Some Reservoir Characteristics, Journal of Petroleum Technology, 146, pp. 55-62. https://doi.org/10.2118/942054-G.

Balaky, S.M., Al-Dabagh, M.M., Asaad, I.Sh., Tamar-Agha, M., Ali, M.S. and. Radwan, A.E., 2023. Sedimentological and Petrophysical Heterogeneities Controls on Reservoir Characterization of the Upper Triassic Shallow Marine Carbonate Kurra Chine Formation, Northern Iraq: Integration of Outcrop and Subsurface Data, Marine and Petroleum Geology, 149, 106085. https://doi.org/10.1016/j.marpetgeo.2022.106085.

Bellen R.C, Dunnigton H.V, Wetzel R. and Morton D.M., 1959. Lexique Stratigraphique International. (3). 333 P.

Buday T., 1980. The Regional Geology of Iraq, Stratigraphy and Paleogeography, Dar Al-Kutub Publication, University of Mosul, Iraq (1).445 P.

Choquette, P.W. and Pray, L.C., 1970. Geologic Nomenclature and Classification of Porosity in Sedimentary Carbonates. AAPG Bull., 54 (2), pp. 207-250. https://doi.org/10.1306/5D25C98B-16C1-11D7-8645000102C1865D.

Csató I., Kiss, K., Toth, S. and Varga, M., 2014. Upper Triassic-Jurassic Depositional Systems in the Akri-Bijeel Exploration Block, Iraqi Kurdistan. MOL Group Scientific Magazine.1. pp. 54-72.

Dresser Atlas, 1979. Long Interpretation Charts: Houston, Dresser Industries, Inc., 107 P.

Fouad, S.F., 2015. Tectonic Map of Iraq, Scale 1: 1000 000, 2012. Iraqi Bulletin of Geology and Mining, 11(1), pp. 1-7. https://ibgm-iq.org/ibgm/index.php/ibgm/article/view/262.

Gulf Keystone Petroleum, 2010. Resource Evaluation of Gulf Keystone's Shaikan. (1-B) Discovery, Kurdistan, Iraq, 50 P.

Hattingh, S., Munn, D., Symms, A., Pocock, N., Wilson, D., Privett, G., Al Marei, K., Ramsay, J., Chernik, P., Ho, J. and Braim, M., 2015. Competent Person's Report on the Interests of Gulf Keystone Petroleum and its Subsidiaries in Kurdistan, Iraq, Gulf Keystone Petroleum, ERC, Iraq, 116 P.

Jassim, S.Z., Buday, T., Cicha, I. and Prouza, V., 2006. Late Permian-Liassic megasequence AP6, In Jassim S.Z., and Goff J.C., 2006 Geology of Iraq. Dolin, Prague and Moravian Museum, Brno, 23 Czech Republic. pp. 124-144.

Jawzi, A. and Associates (AJA), 2005. The Hydrocarbon Potential and Prospectively of Iraq. A Non-Exclusive Report, 1, ECL, Oxon, 160 P.

Kddo, Y.H. and Nader, A.D., 2014. Palynostratigraphy, Age determination and Paleoecology of Butmah Formation in Borehole Kand-1 Northern Iraq. Iraqi National Journal of Earth Sciences, 14(1), pp. 33-48. https://doi.org/10.33899/earth.2014.87486.

Khoshbakht, F., 2015. Evaluating different approaches to permeability prediction in a carbonate reservoir, Journal of Petroleum Science and Technology, 5(1), pp. 79-90. https://doi.org/10.22078/jpst.2015.445.

Larionov, V.V., 1969. Borehole Radiometry. Moscow, U.S.S.R, Nedra, 127 P.

Mohammed Sajed, O.K. and Glover, P.W., 2020. Dolomitisation, Cementation and Reservoir Quality in Three Jurassic and Cretaceous Carbonate Reservoirs in North-Western Iraq, Marine and Petroleum Geology, 115, 104256. https://doi.org/10.1016/j.marpetgeo.2020.104256.

Price, N., LaPointe, P., Parmassar, K., Shi, C., Diamond, P., Finnila, A. and Jensen, O.K., 2020. Dynamic Calibration of the Shaikan Jurassic Full-Field Fractured Reservoir Model Through Single-Well DST and Multi-Well Interference Discrete Fracture Network Simulation, GKP, the Geological Society of London.

Schlumberger, 1972. Log Interpretation–Principles,1, Schlumberger, USA., 113 P.

Schlumberger, 1974. Log Interpretation–Application, 2, Schlumberger, USA., 116 P.

Schlumberger, 1989. Log Interpretation Principles/Applications. Schlumberger, USA.

Selley, R. C., 2000. Applied Sedimentology, (2nd ed.), Academic Press, USA., 521 P.

Silva, F.G.M., Beneduzi, C.F., Nassau, G.F., Rossi, B.T. and Petrobras, P.B.S.A., 2019. Carbonate Porosity and Permeability from Sonic Log, Offshore Technology Conference, OTC, Brazil, 13 P.

Soete, J., Kleipool, L.M., Claes, H., Claes, S., Hamaekers, Kele, S., Ozkul, M., Foubert, A., Reijmer, J.J.G. and Swennen, 2015. Acoustic Properties in Travertines and their Relation to Porosity and Pore Types, Marine and Petroleum Geology, 59, pp. 320-335. https://doi.org/10.1016/j.marpetgeo.2014.09.004.

Tiab, D. and Donaldson, E.C., 2004. Petrophysics, Theory and Practice of Measuring Reservoir Rock and Fluid Transport Properties, Elsevier, INC., 889 P.

Verma, M.K., Ahlbrandt, T.S. and Al-Gailani, M., 2004. Petroleum Reserves and Undiscovered Resources in the Total Petroleum Systems of Iraq: Reserve Growth and Production Implications. GeoArabia, 9 (3), pp. 51-74. https://doi.org/10.2113/geoarabia090351.

Zangana, H.A., Sherwani, G.H., Tawfeeq, T.J. and Al-Ansari, N., 2020. Reservoir Characterization of the Early Jurassic Butmah Formation Using Well Log Data in Selected Wells from Iraqi Kurdistan Region. Open Journal of Geology, 10, pp. 1173-1188. https://doi.org/10.4236/ojg.2020.1012057.